Magnetohydrodynamic Flow and Heat Transfer About a Rotating Disk with Suction and Injection at the Disk Surface

S. Kishore Kumar
William I. Thacker
Layne T. Watson

TR 86-22

MAGNETOHYDRODYNAMIC FLOW AND HEAT TRANSFER ABOUT A ROTATING DISK WITH SUCTION AND INJECTION AT THE DISK SURFACE

S. Kishore Kumar
Director's Unit
National Aeronautical Laboratory
Bangalore India 560 017

William I. Thacker
Computer Science
Winthrop College
Rock Hill, South Carolina 29730

Layne T. Watson *
Departments of Electrical Engineering and Computer Science,
Industrial and Operations Engineering, and Mathematics
University of Michigan
Ann Arbor, Michigan 48109-1092

Abstract. This paper studies the effects of an axial magnetic field on the flow and heat transfer about a porous rotating disk. Using modern quasi-Newton and globally convergent homotopy methods, numerical solutions are obtained for a wide range of magnetic field strengths and injection and suction velocities. Results are presented graphically in terms of three nondimensional parameters. There is excellent agreement with previous work and asymptotic formulas.

1. INTRODUCTION

Von Karman [1] first noted that the Navier-Stokes equations governing the flow past a rotating disk reduced to self similar form. He also obtained an approximate solution for that problem. Later, Cochran [2] obtained a more accurate solution to the same problem. The effects of an axial magnetic field on the flow and heat transfer about a rotating disk were studied by Sparrow and Cess [3]. The pioneering work of Prandtl in 1904 on the mass addition or removal at a bounding surface started continued interest due to its wide range of applications. Some examples are, boundary layer control, cooling of turbine blades, and cooling the skins of high speed aircraft. Considerable work has been done recently on the effects of uniform suction or injection on the flow field induced by a rotating disk. Stuart [4] obtained a series solution for strong suction at the surface of a rotating disk. Sparrow and Gregg [5] developed numerical solutions for the rotating disk problem with suction or injection at the disk surface. Kuiken [6] examined the case of strong injection at the disk surface. Ackroyd [7] obtained uniformly valid series solutions for suction velocities and low values of injection velocities. In this paper we describe the effects of an axial magnetic field and suction (or injection) on the flow and heat transfer about a rotating disk. Pande [8] obtained a series solution for this problem when there is strong suction and a weak magnetic field. We will present results on the flow and heat transfer for a wider range of injection velocities and suction velocities combined with a wide range of magnetic field strengths.

* Research on this paper was completed while Dr. Watson was on sabbatical at the Univeristy of Michigan. Dr. Watson is currently on the faculty of the Computer Science Department at Virginia Tech.

2. GOVERNING EQUATIONS AND BOUNDARY CONDITIONS

Sparrow and Cess [3] discussed, in detail, the assumptions leading to the governing equations of this problem. Therefore, we will not repeat these details. The geometry of the problem being studied is shown in Figure 1. Here (r,θ,z) are cylindrical coordinates, B_0 is the externally applied magnetic field in the z direction, ω is the angular velocity of the disk, T_w is the uniform temperature at the disk surface and T_∞ is the ambient fluid temperature.

In cylindrical coordinates (r,θ,z), assuming angular symmetry, the equations of motion are [3]

$$\rho\left[\left(u\frac{\partial}{\partial r}+w\frac{\partial}{\partial z}\right)u-\frac{v^2}{r}\right]=-\frac{\partial p}{\partial r}-\mu\left(\nabla^2 u-\frac{u}{r^2}\right)-\sigma u B_0^2, \tag{1}$$

$$\rho\left[\left(u\frac{\partial}{\partial r}+w\frac{\partial}{\partial z}\right)v+\frac{uv}{r}\right]=\mu\left(\nabla^2 v-\frac{v}{r^2}\right)-\sigma v B_0^2, \tag{2}$$

$$\rho\left[v\frac{\partial}{\partial r}+w\frac{\partial}{\partial z}\right]w=-\frac{\partial p}{\partial z}+\mu\nabla^2 w, \tag{3}$$

and the continuity equation is

$$\frac{\partial}{\partial r}(ru)+\frac{\partial}{\partial z}(rw)=0, \tag{4}$$

where u, v and w are the velocity components in the r,θ,z directions respectively, ρ is the density of the fluid, μ is the coefficient of viscosity, p is the pressure, σ is the electrical conductivity and

$$\nabla^2=\frac{\partial^2}{\partial r^2}+\frac{1}{r}\frac{\partial}{\partial r}+\frac{\partial^2}{\partial z^2}.$$

The energy equation is

$$\left(u\frac{\partial}{\partial r}+w\frac{\partial}{\partial z}\right)T=\alpha v^2 T, \tag{5}$$

in which T is the static temperature and α is the thermal diffusivity. The boundary conditions of the problem are

$$\left.\begin{aligned}u&=0\\ v&=r\omega\\ w&=-H_w\\ T&=T_w\end{aligned}\right\}\ \text{at } z=0, \qquad \left.\begin{aligned}u&\to 0\\ v&\to 0\\ T&\to T_\infty\end{aligned}\right\}\ \text{as } z\to\infty, \tag{6}$$

where $H_w>0$ corresponds to suction and $H_w<0$ corresponds to injection.

3. REDUCTION TO ORDINARY DIFFERENTIAL EQUATIONS

Following Von Karman [1], we introduce the following relations

$$u=r\omega F(\eta), \qquad v=r\omega G(\eta), \qquad w=(\omega\nu)^{1/2}H(\eta), \tag{7}$$

$$P(\eta)=\frac{p}{\mu\omega}, \qquad \Theta(\eta)=\frac{T-T_\infty}{T_w-T_\infty}, \qquad \eta=z\left(\frac{\omega}{\nu}\right)^{1/2}.$$

Also, from equation (4) we have

$$F(\eta) = -\frac{H'(\eta)}{2}. \tag{8}$$

Substituting equations (7) and (8) into equations (1)-(5), we obtain

$$H''' = HH'' - \frac{(H')^2}{2} + mH' + 2G^2, \tag{9a}$$

$$G'' = HG' - H'G + mG, \tag{9b}$$

$$\Theta'' = Pr H\Theta', \tag{10}$$

where prime denotes differentiation with respect to ν. The Prandtl number Pr and the magnetic parameter m are given by

$$\mathrm{Pr} = \frac{\nu}{\alpha}, \qquad m = \frac{\sigma B_0^2}{\rho\omega}, \tag{11}$$

where $\nu = \mu/\rho$ is the kinematic coefficient of viscosity. In terms of the new variables defined (7), the new boundary conditions from (6) are

$$\left.\begin{aligned} H' &= 0 \\ H &= -A \\ G &= 1 \\ \Theta &= 1 \end{aligned}\right\} \text{ at } \eta = 0, \qquad \left.\begin{aligned} H' &\to 0 \\ G &\to 0 \\ \Theta &\to 0 \end{aligned}\right\} \text{ as } \eta \to \infty, \tag{12}$$

where A is the nondimensional velocity normal to the disk surface. $A > 0$ represents suction while $A < 0$ represents injection. Observe that (10) decouples from (9a) and (9b), and that once $H(\eta)$ has been determined, $\Theta(\eta)$ can be computed by solving a relatively easy one-dimensional two-point boundary value problem.

4. NUMERICAL METHOD

Following the format in Heruska [9], define

$$X = \begin{pmatrix} H''(0) \\ G'(0) \end{pmatrix}. \tag{13}$$

Let $H(\eta; X)$, $G(\eta; X)$ be the solution of the initial value problem given by (9) with the initial conditions (12) and (13). The original two point boundary value problem described by equations (9) and (12) is numerically equivalent to solving the nonlinear system of equations

$$F(X) = \begin{pmatrix} H'(\tau; X) \\ G(\tau; X) \end{pmatrix} = 0, \tag{14}$$

where τ is chosen large enough so that $|H(\eta) - H(\tau)| < \epsilon$ and $|G(\eta) - G(\tau)| < \epsilon$ for $\tau < \eta < \infty$ and a given $\epsilon > 0$. Equation (14) is derived from the boundary conditions (12). Algorithms for solving

non linear systems like (14) typically require partial derivatives such as $\partial H'/\partial X_k$. We can write the functions needed as

$$Y = \left(H(\eta), H'(\eta), H''(\eta), G(\eta), G'(\eta), \frac{\partial H(\eta)}{\partial X_k}, \frac{\partial H'(\eta)}{\partial X_k}, \frac{\partial H''(\eta)}{\partial X_k}, \frac{\partial G(\eta)}{\partial X_k}, \frac{\partial G'(\eta)}{\partial X_k} \right),$$

for $k = 1$ or $k = 2$. Now $H'(\eta; X)$, $G(\eta; X)$ and their partial derivatives can be calculated from the first order system

$$\begin{aligned}
Y_1' &= Y_2 \\
Y_2' &= Y_3 \\
Y_3' &= Y_1 Y_3 - \frac{Y_2^2}{2} + mY_2 + 2Y_4^2 \\
Y_4' &= Y_5 \\
Y_5' &= Y_1 Y_5 - Y_2 Y_4 + mY_4 \\
Y_6' &= Y_7 \\
Y_7' &= Y_8 \\
Y_8' &= Y_1 Y_8 + Y_6 Y_3 - Y_2 Y_7 + 4Y_9 Y_4 + mY_7 \\
Y_9' &= Y_{10} \\
Y_{10}' &= Y_1 Y_{10} + Y_6 Y_5 - Y_7 Y_4 - Y_9 Y_2 + mY_9
\end{aligned} \tag{15a}$$

$$Y(0) = (-A, 0, X_1, 1, X_2, 0, 0, \delta_{1k}, 0, \delta_{2k}) \tag{15b}$$

where δ_{ik} is the Kronecker delta. By solving this system twice, for $k = 1$ and $k = 2$, the Jacobian matrix $DF(X)$ of $F(X)$ can be calculated.

Two methods were utilized to solve this problem, a quasi-Newton method and a globally convergent homotopy method. The quasi-Newton method used was HYBRJ from the MINPACK subroutine package by Argonne National Laboratory [10]. These quasi-Newton routines are robust and quite efficient. However, they fail at times by converging to local minima.

The other method, a globally convergent homotopy method developed by Watson [11], does not suffer from the convergence problems of the quasi-Newton method. However, this method requires considerably more computation time. Details about the algorithm and some of its applications can be found in [11, 12, 13, 14].

The strategy for these problems was to try to solve them first using the inexpensive quasi-Newton method. If that fails, then use the expensive, but guaranteed convergent, homotopy algorithm.

As previously mentioned, these methods use some partial derivatives with respect to the initial conditions. For some values of m and A, these partials increase drastically as η increases. This problem was worse in cases where m was large and/or there was large injection velocity. Large values of suction velocity tended to make the problem better conditioned. Therefore, results with large m and/or large injection velocities are not as accurate as other results. This also limited the range of injection velocities and m values for which solutions could be computed. Such instability is an inherent problem with shooting methods, the type used. Other methods, such as finite difference, collocation, and finite element, will be considered in future work.

5. DISCUSSION

The flow depends on two parameters, A and m, while the temperature depends on Pr, A and m. Graphs are presented to gain some insight into the effects of these parameters. For $m = 0$ we have the case of a rotating disk in the absence of a magnetic field while $A = 0$ corresponds to the case of an impermeable rotating disk. The effects of A and m on radial velocity ($F(\eta)$) are shown in Figures 2 and 3. From these figures, we see that the radial velocity increases monotonically with increased η, until a maximum is reached, and then decreases monotonically to 0 as $\eta \to \infty$. For an imposed magnetic field, as the value of suction decreases (Figure 2), the maximum for radial velocity moves away from the disk and the magnitude of the radial velocity increases. Increasing the value for injection moves the maximum away from the disk and increases the maximum away from the disk and increases the maximum radial velocity. For an imposed suction value, as the strength of the magnetic field increases (Figure 3), the maximum radial velocity moves towards the disk and the magnitude of this maximum decreases. From these two figures, it can be inferred that for large values of m, there is a considerable reduction in the three dimensional character of radial velocity (i.e., the flow becomes two dimensional).

Figures 4, 5 and 6 show the behavior of the tangential velocity ($G(\eta)$) for various values of A and m. For an imposed magnetic field, as suction increases (Figure 4), the boundary layer thickness increases, whereas an opposite effect is observed for increasing injection values. Figures 5 and 6 show the effects of various magnetic fields on the tangential velocity for $A = 1.0$ and -1.0. In both cases the increase in magnetic field has the same effect as that of suction, namely thinning of the boundary layer.

Figure 7 shows that with an imposed magnetic field, for higher values of suction the axial velocity is almost constant with respect to η. When A is -1.0, there is still some inflow in the axial direction at infinity. But, as the injection values increase (-2, -3), there is no inflow as all. We can understand this better by referring to Table 1. For $m = 0.1$ there is inflow towards the disk in the axial direction from infinity ($H(\infty)$ is negative) for all values of injection. For $m = 0.5$ there is no inflow from infinity ($H(\infty)$ is positive) when the injection value has a larger magnitude than -2.0. The effect of m on H can be seen from Figure 8 and Table 1. For small values of suction, as the strength of the magnetic field increases, the axial flow towards the disk decreases. For larger values of suction ($A > 2.0$), the increase in magnetic field has less effect on $H(\infty)$. For small injection values ($A = -0.1$), $H(\infty)$ becomes positive when $m = 4.0$; for $A = -0.5$ onwards, $H(\infty)$ becomes positive for smaller values of m.

The torque (M) required to overcome the shear on one side of the disk is given by

$$\frac{2M}{\pi r_0^4 \rho (\nu\omega^3)^{1/2}} = -G'(0), \tag{16}$$

where r_0 is the radius of the disk. The effect of m and A on $G'(0)$ can be observed from Table 1. The torque on the disk increases with m for all values of A. However, when suction is small, say $A = 0.1$, $G'(0)$ increases by nearly 192% as m increases from 0.1 to 4.0 . Contrast this with the case $A = 5.0$, where the increase is only 13.5% as m increases from 0.1 to 4.0 . This shows that while the effect of m on torque is large when suction is small, the effect is reduced as suction increases. Table 1 also shows that as the values for injection increase in magnitude, the effect of m on torque becomes increasingly dominant.

6. DISPLACEMENT THICKNESS AND MOMENTUM THICKNESS

For the tangential direction, define the displacement thickness δ^* as

$$\delta^* \left(\frac{\omega}{\nu}\right)^{1/2} = \int_0^\infty G(\eta) d\eta. \tag{17}$$

The momentum thickness for the flow about a rotating disk as defined by Stuart [4] is

$$\delta_1^* \left(\frac{\omega}{\nu}\right)^{1/2} = \int_0^\infty G(\eta)(1 - G(\eta)) d\eta. \tag{18}$$

The values obtained for δ^* and δ_1^* are shown in Table 1 as functions of m and A. The displacement thickness decreases for increased suction and increases for increased injection. The displacement thickness is greatly affected by increasing m when the suction value is small, whereas the displacement thickness changes only slightly with increases in m when the suction values get larger. However, for all values of injection, displacement thickness decreases significantly with increased m. Similar trends are observed for momentum thickness.

7. HEAT TRANFER

From Fourier's Law, the heat transfer from the disk to the fluid in transformed variables is

$$q = -\kappa (T_w - T_\infty) \left(\frac{\omega}{\nu}\right)^{1/2} \Theta'(0), \tag{19}$$

where κ is the thermal conductivity. The Nusselt number is given by

$$\mathrm{Nu} = \frac{q (\nu/\omega)^{1/2}}{(T_w - T_\infty)\kappa}. \tag{20}$$

From (19) and (20)

$$\mathrm{Nu} = -\Theta'(0). \tag{21}$$

An expression for $-\Theta'(0)$ is obtained by integrating equation (10) subject to the boundary conditions (12) resulting in:

$$-\Theta'(0) = \frac{1}{\displaystyle\int_0^\infty \exp\left[\mathrm{Pr}\int_0^\xi H(\eta) d\eta\right] d\xi}. \tag{22}$$

Some values of $-\Theta'(0)$ obtained from the above integration are shown in Tables 2 and 3. We can see that the Nusselt number $(-\Theta'(0))$ increases as suction increases but decreases as injection increases. For a given A, Nu increases as Pr increases. From Table 3, we can see that for $A = 1.0$, an increase in m from 0 to 4.0 decreases Nu by less than 19% for Pr=0.01 and by less than 0.4% for Pr=10.0 .

Values could not be obtained for Nu with A and m parameters that result in a $H(\infty)$ value greater than 0. Such values cause the integration in the $-\Theta'(0)$ equation to diverge.

Tables 4 and 5 show good agreement of our results with the analytical solution obtained by Pande[8] for large A and small m and the numerical results of Sparrow and Gregg[5] for $m = 0$.

8. ASYMPTOTIC COMPARISONS

Applying standard perturbation techniques to the equations in (9) for small A and large m gives the asymptotic formulas

$$H = \frac{2}{3m^{3/2}}\left[e^{-\sqrt{m}\eta} - \frac{1}{2}e^{-2\sqrt{m}\eta} - \frac{1}{2}\right] - A, \tag{23}$$

$$-H(\infty) = \frac{1}{3m^{3/2}} + A. \tag{24}$$

From Table 6, we see that the asymptotic formula for $H(\infty)$ is fairly accurate for m values as low as 2. Also, as A increases, the percent difference decreases even though the absolute difference increases. However, negative values of A have a larger difference as well as a larger percent difference as the magnitude increases. The asymptotic formula does not have as much accuracy with injection values as it does for suction.

A	m	$H''(0)$	$G'(0)$	$H(\infty)$	$\delta^*(\omega/\nu)^{1/2}$	$\delta_1^*(\omega/\nu)^{1/2}$
0.1	0.1	-.94970031	-0.70556753	-0.80728	1.1888	0.56923
0.1	0.5	-.75941834	-0.89547865	-0.51409	1.0308	0.50523
0.1	1.0	-.61001359	-1.1179265	-0.33015	0.86351	0.42797
0.1	2.0	-.45588843	-1.4921873	-0.20045	0.66254	0.33033
0.1	4.0	-.32862435	-2.0606763	-0.13849	0.48375	0.24168
0.5	0.1	-.87549736	-0.90682387	-0.95198	1.0012	0.48878
0.5	0.5	-.69933108	-1.1086137	-0.76389	0.86247	0.42644
0.5	1.0	-.56725454	-1.3356967	-0.65346	0.73299	0.36456
0.5	2.0	-.43130013	-1.7095775	-0.57285	0.58047	0.28968
0.5	4.0	-.31608844	-2.2746559	-0.53043	0.43859	0.21917
1.0	0.1	-.73348580	-1.2305623	-1.2269	0.78192	0.38723
1.0	0.5	-.60106000	-1.4357645	-1.1410	0.68282	0.33973
1.0	1.0	-.50208794	-1.6570758	-1.0898	0.59708	0.29775
1.0	2.0	-.39513646	-2.0184735	-1.0481	0.49318	0.24631
1.0	4.0	-.29803228	-2.5693250	-1.0225	0.38858	0.19421
2.0	0.1	-.46957149	-2.0834812	-2.0536	0.47727	0.23830
2.0	0.5	-.42074136	-2.2490111	-2.0413	0.44289	0.22123
2.0	1.0	-.37743805	-2.4313615	-2.0318	0.41017	0.20494
2.0	2.0	-.32102279	-2.7423451	-2.0213	0.36407	0.18197
2.0	4.0	-.25887694	-3.2413392	-2.0123	0.30828	0.15411
3.0	0.1	-.32592346	-3.0445028	-3.0175	0.32804	0.16397
3.0	0.5	-.30740555	-3.1678635	-3.0153	0.31534	0.15763
3.0	1.0	-.28844315	-3.3105664	-3.0131	0.30180	0.15087
3.0	2.0	-.25964084	-3.5671320	-3.0102	0.28017	0.14006
3.0	4.0	-.22194538	-4.0034081	-3.0069	0.24970	0.12484
4.0	0.1	-.24719169	-4.0298749	-4.0076	0.24804	0.12401
4.0	0.5	-.23870361	-4.1258146	-4.0070	0.24229	0.12113
4.0	1.0	-.22932912	-4.2400206	-4.0064	0.23577	0.11788
4.0	2.0	-.21370296	-4.4526459	-4.0054	0.22452	0.11226
4.0	4.0	-.19061247	-4.8306252	-4.0041	0.20698	0.10348
5.0	0.1	-.19864430	-5.0225310	-5.0039	0.19907	0.099530
5.0	0.5	-.19413489	-5.1005006	-5.0037	0.19603	0.098010
5.0	1.0	-.18894688	-5.1948049	-5.0035	0.19247	0.096232
5.0	2.0	-.17980709	-5.3741780	-5.0031	0.18605	0.093023
5.0	4.0	-.16516062	-5.7030098	-5.0025	0.17533	0.087663
0.0	0.1	-.96096043	-0.66211964	-0.77929	1.2363	0.58847
0.0	0.5	-.77026519	-0.84872385	-0.45888	1.0755	0.52567
0.0	1.0	-.61851596	-1.0690534	-0.25331	0.89896	0.44505
0.0	2.0	-.46111824	-1.4420940	-0.10858	0.68477	0.34131
0.0	4.0	-.33140610	-2.0102667	-0.040775	0.49577	0.24767

A	m	$H''(0)$	$G'(0)$	$H(\infty)$	$\delta^*(\omega/\nu)^{1/2}$	$\delta_1^*(\omega/\nu)^{1/2}$
-0.1	0.1	-.96927842	-0.62109785	-0.75394	1.2839	0.60729
-0.1	0.5	-.77923730	-0.80441572	-0.40639	1.1210	0.54628
-0.1	1.0	-.62598320	-1.0223583	-0.17809	0.93547	0.46256
-0.1	2.0	-.46591593	-1.3937003	-0.017229	0.70768	0.35262
-0.1	4.0	-.33402817	-1.9610945	0.056832	0.50807	0.25381
-0.5	0.1	-.97523069	-0.47860730	-0.67365	1.4764	0.67862
-0.5	0.5	-.79618949	-0.64963677	-0.22074	1.3106	0.62967
-0.5	1.0	-.64470132	-0.85634630	0.10702	1.0912	0.53644
-0.5	2.0	-.48031949	-1.2168142	0.34294	0.80587	0.40097
-0.5	4.0	-.34276608	-1.7766978	0.44613	0.56019	0.27976
-1.0	0.1	-.93342121	-0.34145130	-0.60563	1.7252	0.76046
-1.0	0.5	-.77949348	-0.49935791	-0.032133	1.5623	0.73459
-1.0	1.0	-.64332440	-0.69066292	0.43166	1.3048	0.63569
-1.0	2.0	-.40244571	-1.3204110	0.78156	0.94240	0.46784
-1.0	4.0	-.34935998	-1.5731223	0.93015	0.63162	0.31531
-2.0	0.1	-.76986197	-0.17012160	-0.52194	2.2707	0.91238
-2.0	0.5	-.67355551	-0.30469715	0.25947	2.1129	0.94692
-2.0	1.0	-.58296165	-0.46571471	1.0075	1.7822	0.85028
-2.0	2.0	-.46608986	-0.75841319	1.6265	1.2534	0.61869
-2.0	4.0	-.34797800	-1.2471552	1.8900	0.79339	0.39564
-3.0	0.1	-.60318822	-0.08888757	-0.46554	2.8897	1.0652
-3.0	0.5	-.54997174	-0.20059342	0.49926	2.7237	1.1693
-3.0	1.0	-.49679764	-0.33393640	1.5417	2.3084	1.0790
-3.0	2.0	-.42062178	-0.58053840	2.4462	1.5974	0.78175
-3.0	4.0	-.33145553	-1.0093864	2.8415	0.97518	0.48542
-4.0	0.1	-.47811827	-0.05236093	-0.41853	3.5666	1.2289
-4.0	0.5	-.44915707	-0.14412499	0.74209	3.3743	1.3991
-4.0	1.0	-.41848145	-0.25452370	2.1621	2.7973	1.2495
-4.0	2.0	-.37057638	-0.46234394	3.2866	1.9269	0.91705
-4.0	4.0	-.30710176	-0.83580028	3.7894	1.1667	0.57715

Table 1 Effect of A and m on Torque $(G'(0))$; axial velocity at infinity $(H(\infty))$; displacement thickness (δ^*) and momentum thickness (δ_1^*).

A\Pr	0.01	0.10	1.0	10.0
4.0	0.040069	0.4006091	4.002395	40.00112
3.0	0.030151	0.3013329	3.005322	30.00255
2.0	0.024076	0.2036261	2.015051	20.00770
1.0	0.011394	0.1126061	1.059119	10.03991
0.0	0.004556	0.0428310	0.2826559	.9515366
-1.0	0.000318	0.0031799	0.0034330	

Table 2. Effect of Prandtl number (Pr) and A on Nusselt number $\mathrm{Nu} = -\Theta'(0)$ when $m = .5$.

$m \backslash \mathrm{Pr}$	0.01	0.10	1.0	10.0
0.0	0.012566	0.1225589	1.0925388	10.054518
0.5	0.011394	0.1126061	1.0591194	10.039911
1.0	0.010889	0.1081711	1.0418339	10.031811
2.0	0.010477	0.1044617	1.0254037	10.023168
3.0	0.010311	0.1029297	1.0177857	10.018525
4.0	0.010224	0.1021232	1.0134742	10.015565

Table 3. Effect of m and Pr on Nu when $A = 1.0$.

A	$-H(\infty)^*$	$-H(\infty)^{**}$
2.	2.0533	2.0536
3.	3.0175	3.0175
4.	4.0076	4.0076
5.	5.0039	5.0039

Table 4. Comparison of the analytic solution of Pande [8] (* column) and the present numerical results (** column; comparison valid only for large suction (A) and small m). $m = .1$.

A	$-H''(0)^*$	$-H''(0)^{**}$	$-G'(0)^*$	$-G'(0)^{**}$
4.0	0.2495	0.249475	4.005	4.00518
2.0	0.4848	0.484832	2.039	2.03853
0.0	1.020	1.02047	0.6159	0.615922
-1.0	0.9790	0.978962	0.3022	0.302173
-5.0	0.395	0.395131	0.0155	0.015471

Table 5. Comparison of the numerical solutions from Sparrow and Gregg [5] (* column) and the present numerical results (** column).

A	m	$-H(\infty)_{\text{obt}}$	$-H(\infty)_{\text{asy}}$	|dif|	% |dif|
0.0	1.0	0.25331	0.33333	0.08002	24.0
0.0	2.0	0.10858	0.11785	0.00927	7.8
0.0	4.0	0.04078	0.04172	0.00094	2.3
1.0	1.0	1.0898	1.3333	0.2435	18.3
1.0	2.0	1.0481	1.1178	0.0697	6.2
1.0	4.0	1.0225	1.0417	0.0192	1.8
2.0	1.0	2.0318	2.3333	0.3015	12.9
2.0	2.0	2.0213	2.1178	0.0965	4.6
2.0	4.0	2.0123	2.0417	0.0294	1.4
3.0	1.0	3.0131	3.3333	0.3202	9.6
3.0	2.0	3.0102	3.1178	0.1076	3.5
3.0	4.0	3.0069	3.0417	0.0348	1.1
-1.0	1.0	-0.43166	-0.6667	0.23504	35.3
-1.0	2.0	-0.78157	-0.8822	0.10063	11.4
-1.0	4.0	-0.93015	-0.9583	0.02815	2.9
-2.0	1.0	-1.0070	-1.6667	0.6597	39.6
-2.0	2.0	-1.6265	-1.8822	0.2557	13.6
-2.0	4.0	-1.8900	-1.9583	0.0683	3.5
-3.0	1.0	-1.5417	-2.6667	1.1250	42.2
-3.0	2.0	-2.4462	-2.8822	0.4360	15.1
-3.0	4.0	-2.8415	-2.9583	0.1168	3.9

Table 6 . Comparison of obtained values with asymptotic formula values.

References

1. T. Von Karman, Uber Laminare und Turbulente Reibung. *ZAMM* **1**, 233–252 (1921).

2. W. G. Cochran, The Flow Due to a Rotating Disk. *Proc. Camb. Phil. Soc.* **30**, 365–375 (1934).

3. E. M. Sparrow and R. D. Cess, Magnetohydrodynamic and Heat Transfer about a Rotating Disk. *J. Appl. Mech.* **29**, 181–187 (1962).

4. J. T. Stuart, On the Effects of Uniform Suction on the Steady Flow due to a Rotating Disk. *Quart. J. Mech. Appl. Math.* **7**, 446–457 (1954).

5. E. M. Sparrow and J. L. Gregg, Mass Transfer and Heat Transfer about a Rotating Disk. *ASME J. Heat Trans.* **81**, 294–302 (1959).

6. H. K. Kuiken, The Effect of Normal Blowing on the Flow near a Rotating Disk of Infinite Extent. *J. Fluid Mech.* **47**, 789–798 (1971).

7. J. A. D. Ackroyd, On the Steady Flow Produced by a Rotating Disk with Either Surface Suction or Injection. *J. Engng. Math* **12**, 207–209 (1978).

8. G. S. Pande, On the Effects of Uniform High Suction on the Steady MDH Flow Due to a Rotating Disk. *Appl. Sci. Res.* **11**, 205–212 (1972).

9. M. W. Heruska, Micropolar Flow past a Porous Stretching Sheet. *M.S. Thesis*, Dept. of Computer Science, Virginia Polytechnic Institute and State University, Blacksburg, Va., Oct., 1984.

10. J. J. Moré, B. S. Garbow and K. E. Hillstrom, User Guide for MINPACK-1. ANL-80-74, Argonne National Laboratory, (1980).

11. L. T. Watson, A Globally Convergent Algorithm for Computing Fixed Points of C^2 Maps. *Appl. Math. Comput.* **5**, 297–311 (1979).

12. L. T. Watson, Numerical Study of Porous Channel flow in a Rotating system by a Homotopy Method. *J. Comput. Appl. Math* **7**, 21–26 (1981).

13. L. T. Watson, and D. Fenner, Chow-Yorke Algorithm for Fixed Points or Zeros of C^2 Maps. *ACM Trans. Math. Software* **6**, 252–259 (1980).

14. L. T. Watson, Engineering applications of the Chow-Yorke Algorithm. *Appl. Math. Comput.* **9**, 111–133 (1981).

Figure Captions

Figure 1. Coordinate system.

Figure 2. Effect of A on radial velocity F. A = -3.0, -2.0, -1.0, 0.0, 1.0, 2.0, 3.0, 4.0 (top to bottom), $m = .5$.

Figure 3. Effect of m on radial velocity F. m = 0.0, 0.1, 0.5, 1.0, 2.0, 3.0, 4.0 (top to bottom), $A = 1.0$.

Figure 4. Effect of A on tangential velocity G. A = -3.0, -2.0, -1.0, 0.0, 1.0, 2.0, 3.0, 4.0 (top to bottom), $m = .5$.

Figure 5. Effect of m on tangential velocity G for imposed suction. m = 0.0, 0.1, 0.5, 1.0, 2.0, 3.0, 4.0 (top to bottom), $A = 1.0$.

Figure 6. Effect of M on tangential velocity G for imposed injection. m = 0.0, 0.1, 0.5, 1.0, 2.0, 3.0 (top to bottom). $A = -1.0$.

Figure 7. Effect of A on axial velocity H. A = -3.0, -2.0, -1.0, 0.0, 1.0, 2.0, 3.0, 4.0 (top to bottom), $m = 0.5$.

Figure 8. Effect of m on axial velocity H. m = 4.0, 3.0, 2.0, 1.0, 0.5, 0.1, 0.0 (top to bottom), $A = 1.0$.

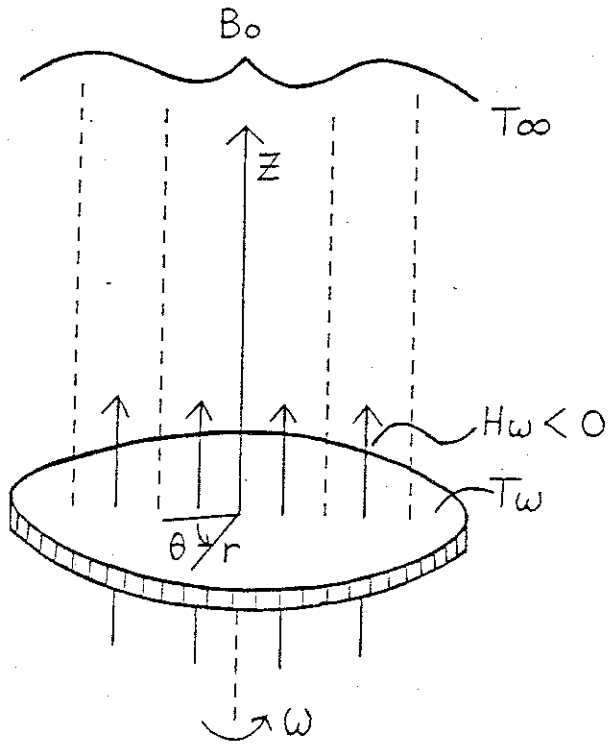

Fig. 1

Fig 2

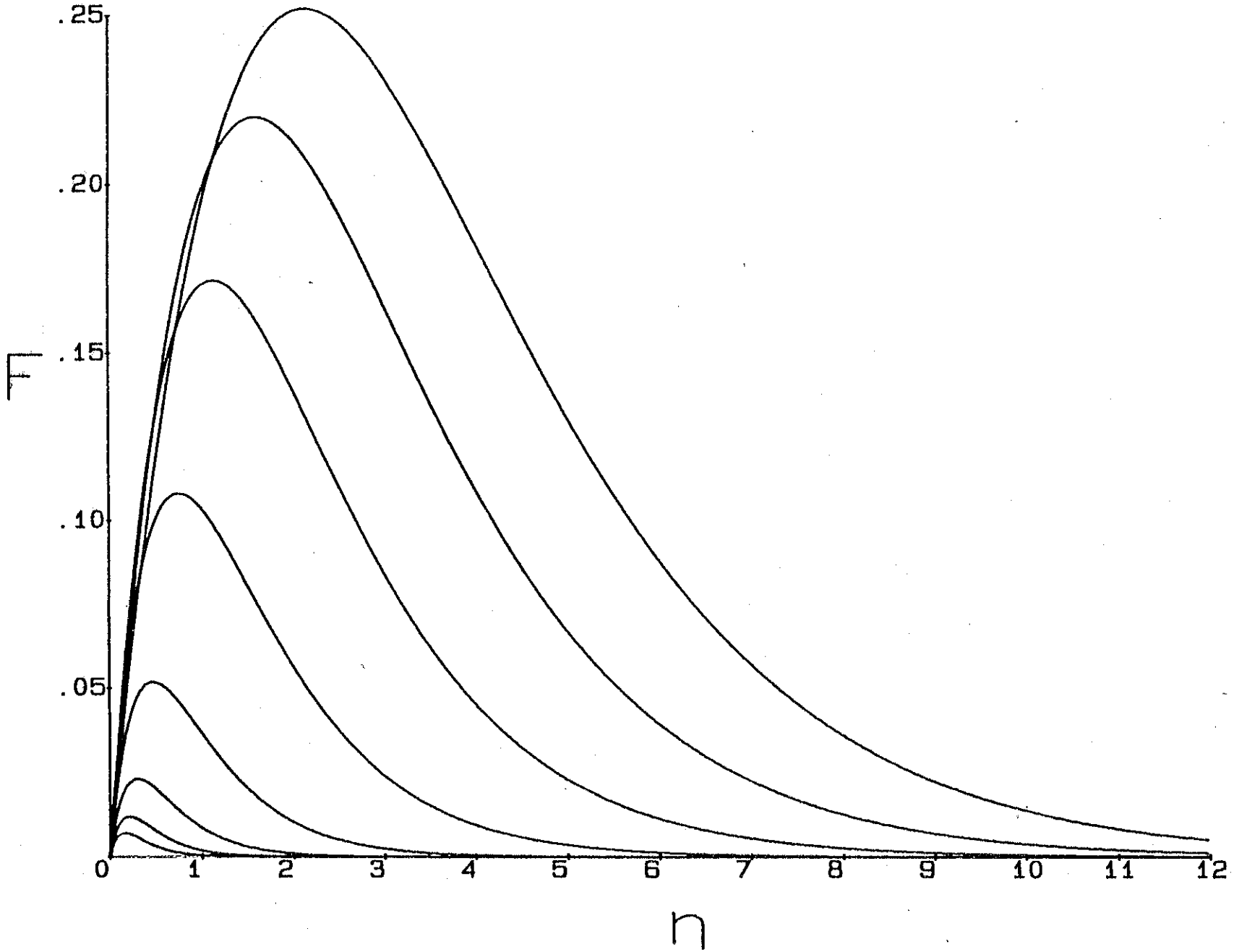

Fig 3

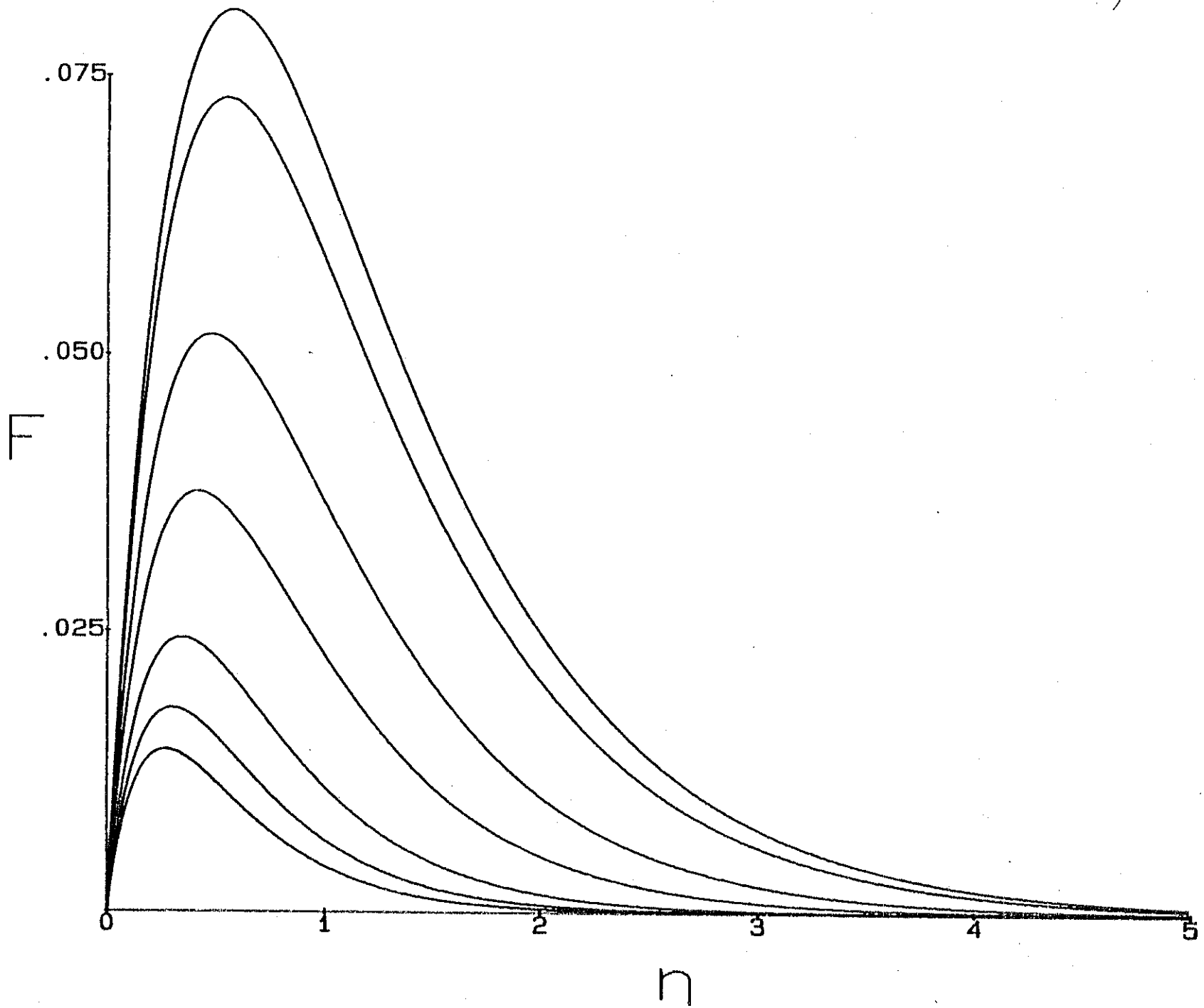

Fig 4

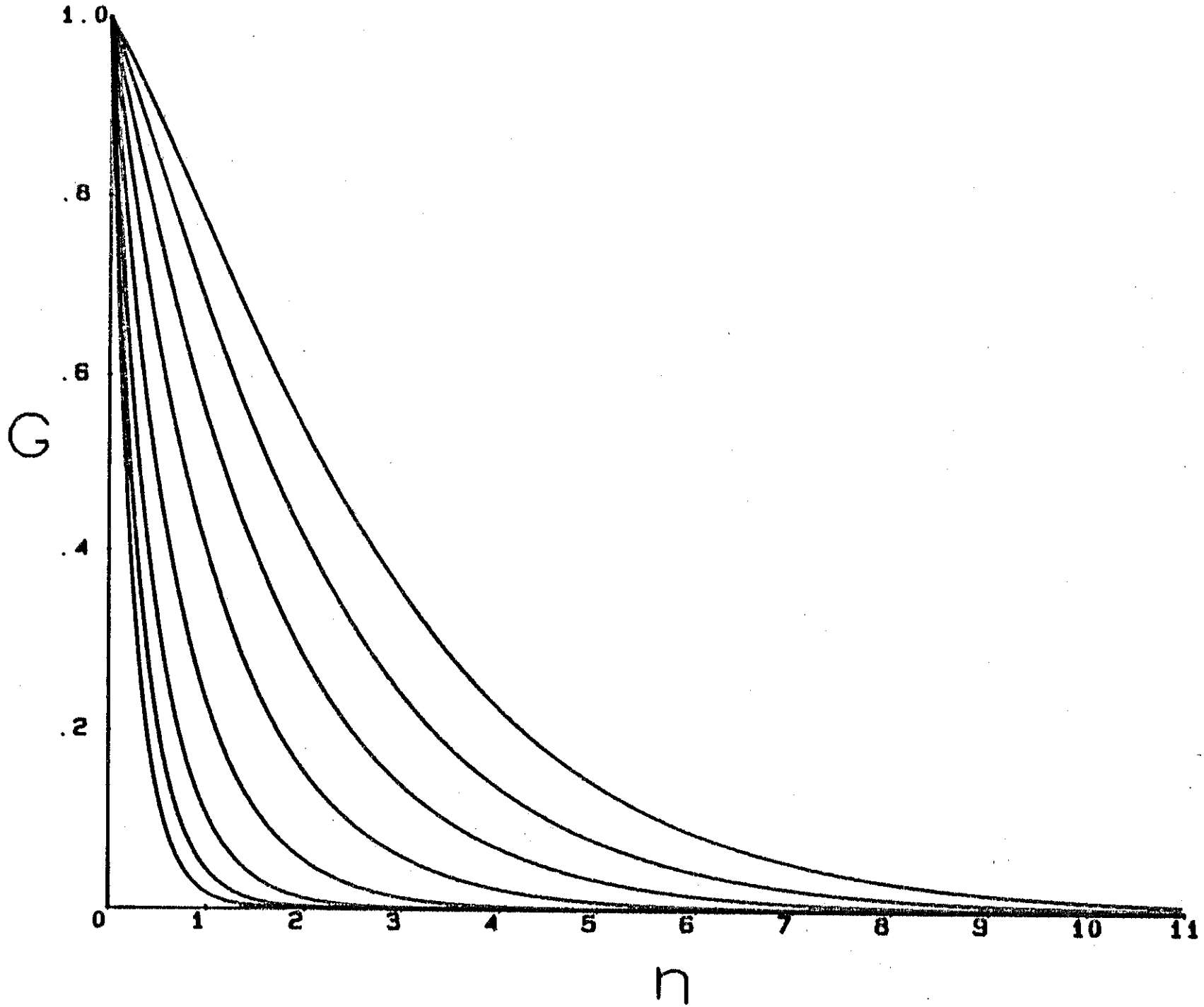

Fig 5

Fig 6

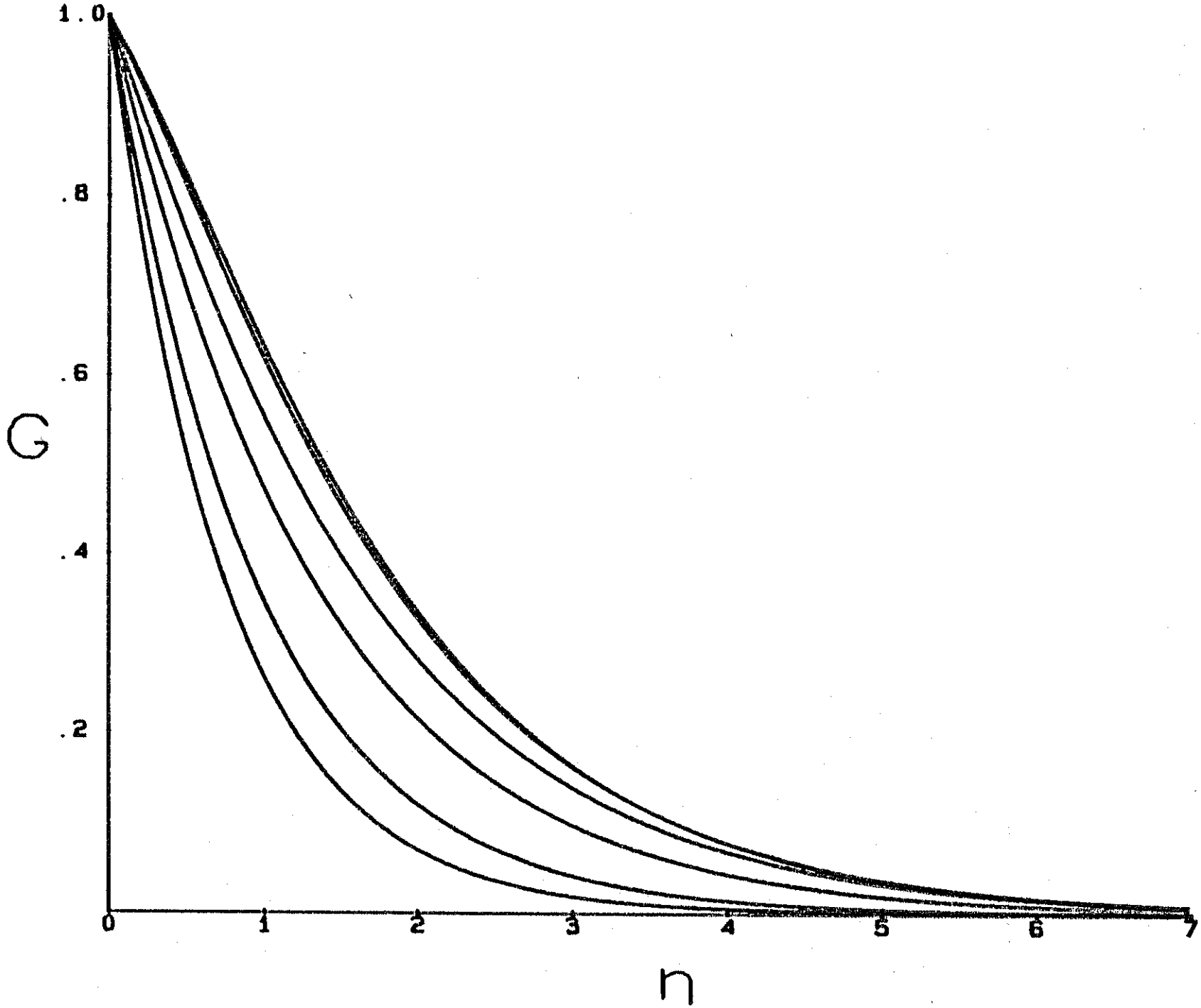

Fig 7

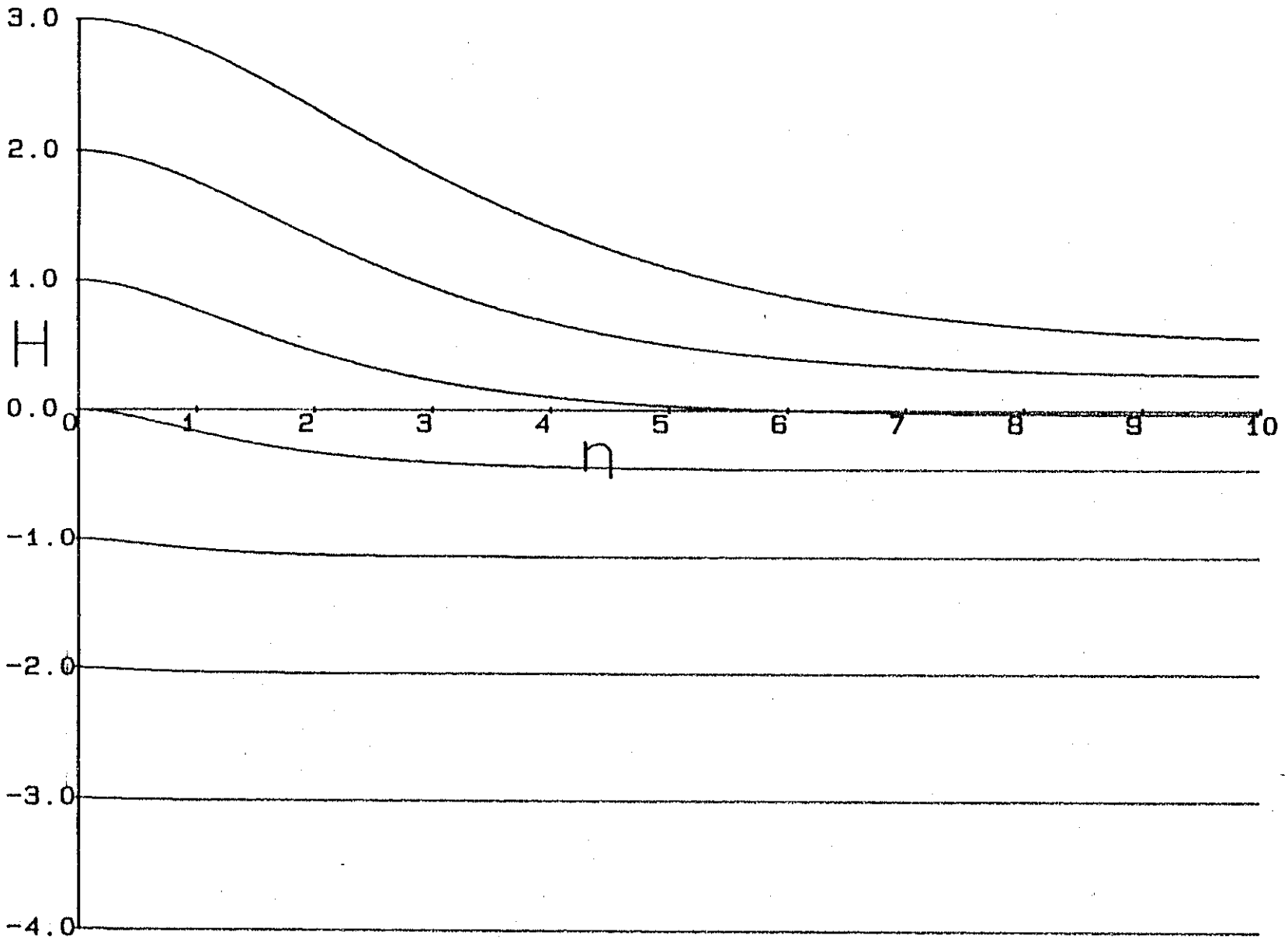

Fig 8